

# A mesocortical dopamine circuit enables the cultural transmission of vocal behaviour

著者	Masashi Tanaka, Fangmiao Sun, Yulong Li, Richard Mooney
journal or publication title	Nature
volume	563
page range	117-120
year	2018-10-17
URL	<a href="http://hdl.handle.net/10097/00125837">http://hdl.handle.net/10097/00125837</a>

doi: 10.1038/s41586-018-0636-7

1 **A mesocortical dopamine circuit enables the cultural transmission of vocal behavior**

2

3 Masashi Tanaka<sup>1,2</sup>, Fangmiao Sun<sup>3,4</sup>, Yulong Li<sup>3,4,5</sup>, and Richard Mooney<sup>1\*</sup>

4

5 <sup>1</sup>Department of Neurobiology, Duke University, Durham, NC 27710 USA

6 <sup>2</sup>Present Address: Graduate School of Life Sciences, Tohoku University, Sendai, Miyagi 980-  
7 8577 Japan

8 <sup>3</sup>State Key Laboratory of Membrane Biology, Peking University School of Life Sciences,  
9 Beijing 100871, China

10 <sup>4</sup>PKU-IDG/McGovern Institute for Brain Research, Beijing 100871, China

11 <sup>5</sup>Peking-Tsinghua Center for Life Sciences, Beijing 100871, China

12

13 \*Correspondence: [mooney@neuro.duke.edu](mailto:mooney@neuro.duke.edu)

14 **The cultural transmission of behavior depends on a pupil's ability to identify and emulate**  
15 **an appropriate tutor<sup>1-4</sup>. How the pupil's brain detects a suitable tutor and encodes the**  
16 **tutor's behavior is largely unknown. Juvenile zebra finches readily copy songs of adult**  
17 **tutors they interact with, but not songs they listen to passively through a speaker<sup>5,6</sup>,**  
18 **indicating that social cues generated by the tutor facilitate song imitation. Here we show**  
19 **that neurons in the midbrain periaqueductal gray (PAG) of juvenile finches are selectively**  
20 **excited by a singing tutor and, by releasing dopamine (DA) in a sensorimotor cortical**  
21 **analogue (HVC), help encode tutor song representations used for vocal copying. Blocking**  
22 **DA signaling in the pupil's HVC during tutoring blocked copying, whereas pairing**  
23 **stimulation of PAG terminals in HVC with song played through a speaker was sufficient**  
24 **to drive copying. Exposure to a singing tutor triggered the rapid emergence of responses**  
25 **to the tutor song in the pupil's HVC and a rapid increase in the pupil's song complexity,**  
26 **an early signature of song copying<sup>7,8</sup>. These findings reveal that a dopaminergic**  
27 **mesocortical circuit detects a tutor's presence and helps encode the tutor's performance,**  
28 **facilitating the cultural transmission of vocal behavior.**

29

30 The cortical song nucleus HVC is crucial to singing and song learning<sup>7,9-12</sup> and receives  
31 convergent input from premotor, auditory, and neuromodulatory afferents, including dopamine  
32 (DA)-secreting neurons in the midbrain periaqueductal gray (PAG)<sup>13-15</sup> (Fig. 1a-c, Extended  
33 Data Fig. 1a-c). In the mammalian PAG, DA neurons encode information about social context,  
34 arousal in response to behaviorally salient stimuli, or reward<sup>16-18</sup>, raising the possibility that the  
35 PAG to HVC pathway in juvenile finches encodes information about the tutor that facilitates  
36 song imitation. To explore this idea, we implanted tetrodes into the PAG of juvenile male  
37 finches raised in isolation from a tutor (tutor-naive juveniles; see Methods) (Fig. 1d-k). Most  
38 PAG neurons (81.8%: 18/22 neurons from 4 birds) increased their action potential activity in  
39 the presence of a singing tutor (Fig. 1e-g, k), whereas PAG activity was unaffected during  
40 encounters with non-singing adult male finches or female finches, which do not sing (Fig. 1i-  
41 j, k). Neural activity in the juvenile's PAG was not precisely locked to syllables of the tutor  
42 song, was variable across different tutor song bouts, and could remain elevated for hundreds of  
43 milliseconds after the tutor stopped singing (Extended Data Fig. 2c-f), suggesting that PAG  
44 activity evoked by a singing tutor is not simply auditory in nature. Indeed, playback of adult  
45 finch song from a speaker, including that of a recent tutor, failed to evoke activity in the  
46 juvenile's PAG (Fig. 1h, k). Moreover, song playback from a speaker in the presence of an  
47 adult female bird failed to activate PAG neurons in tutor-naive juveniles (Extended Data Fig.  
48 2a,b). Therefore, PAG neurons in juvenile males respond strongly and selectively to a live

49 singing tutor and thus can signal the presence of a suitable song model.

50 These findings raise the possibility that experience of a singing tutor stimulates DA release  
51 from PAG terminals in HVC. We explored this idea by virally expressing a modified dopamine  
52 type 2 (D2) receptor in HVC neurons of tutor-naive juvenile males that increases fluorescence  
53 upon DA binding (Fig. 2) (AAV 2/9.hSyn.GRAB<sub>DA1h</sub>)<sup>19</sup>. We then head-fixed these juvenile  
54 males in the awake state and used two-photon imaging methods<sup>20</sup> to establish that DA levels in  
55 HVC increase in the presence of a singing tutor (Fig. 2c-d, i). In contrast, DA-related changes  
56 in fluorescence were not detected in the juvenile's HVC in response to song playback (Fig. 2e,  
57 i), or when the juvenile encountered non-singing adult males or females (Fig. 2f, g, i),  
58 paralleling the selective enhancement of PAG activity elicited by a singing tutor. Moreover,  
59 ablating DA neurons in the pupil's PAG with 6-hydroxydopamine (6-OHDA<sup>21</sup>) prevented tutor-  
60 evoked DA transients in the pupil's HVC (Fig. 2h, i), confirming that tutor-evoked DA release  
61 in the pupil's HVC largely originates from the PAG.

62 To explore whether DA signaling in HVC plays a role in song imitation, we used 6-OHDA to  
63 lesion DA-releasing fibers in the HVC of juvenile male finches raised continuously with adult  
64 male tutors and tracked their song development into adulthood (Fig. 3a-c, Extended Data Fig.  
65 3). Lesions of DA-releasing fibers in HVC made near the onset of the sensitive period for tutor  
66 song memorization (30 days-post-hatch<sup>22</sup> or 30 d) prevented song copying (Fig. 3d-e) without

67 affecting the overall rate of singing (Extended Data Fig. 4a). As adults, these 6-OHDA treated  
68 birds produced abnormally long and acoustically simple syllables, similar to finches raised in  
69 isolation from a tutor<sup>22</sup> (Extended Data Fig. 4b, c). The 6-OHDA lesions made in HVC in 30 d  
70 males are permanent and thus could potentially interfere with tutor song memorization (i.e.,  
71 sensory learning), the subsequent phase of song copying (sensorimotor learning), or both.  
72 However, 6-OHDA lesions made in the HVC of 45 d males, which have had sufficient tutor  
73 experience to enable accurate copying but are just beginning sensorimotor learning<sup>22</sup>, did not  
74 affect the juvenile's ability to copy a tutor song (Fig. 3d, f).

75 These findings suggest that DA signaling in HVC plays a role in sensory learning but cannot  
76 exclude a more general but developmentally restricted (before 45d, e.g.) role for such signaling.  
77 Therefore, we used microdialysis methods<sup>23</sup> to reversibly block DA receptors in the HVC<sup>24</sup> of  
78 tutor-naïve juvenile males (Age:  $43.0 \pm 4.9$  d [mean  $\pm$  SD],  $n = 5$ ) while they were housed with  
79 a tutor for 1.5 h on five consecutive days, allowing us to better determine whether DA signaling  
80 in HVC is crucial during pupil-tutor interactions, when sensory learning occurs (Fig. 3g-h,  
81 Extended Data Fig. 5a-c). Reversibly blocking DA receptors in HVC during but not just after  
82 tutoring sessions blocked song copying (Fig. 3h, Extended Data Fig. 5b-c), without affecting  
83 juveniles' attentive behaviors to tutors or tutors' singing rates (Extended Data Fig. 5d-e,  
84 Supplementary Video 1-2). Moreover, reversibly suppressing PAG activity in the pupil with  
85 muscimol during daily tutoring sessions also blocked song copying; notably, juveniles in which

86 PAG was inactivated also failed to orient to their tutors, even though tutors continued singing  
87 at normal rates (Extended Data Fig. 5d-h, Supplementary Video 3). Thus, tutor-evoked  
88 activation of the pupil's PAG and concomitant release of DA in HVC are essential to encoding  
89 tutor song experience, and PAG activity may be required for the pupil to attend to a singing  
90 tutor.

91 The current findings do not exclude the possibility that DA signaling at other sites also  
92 contributes to sensory learning. One potential site is the basal ganglia region Area X<sup>11</sup>, which  
93 receives dopaminergic input from the ventral tegmental area and substantia nigra pars compacta  
94 (VTA/SNc), as well as from a smaller cohort of TH+ PAG neurons (Extended Data Fig. 1d-g),  
95 and where dopamine signaling plays a role in sensorimotor learning<sup>25</sup>. Nonetheless, infusing  
96 DA receptor blockers into Area X of juvenile males during daily tutoring sessions did not affect  
97 song copying (Extended Data Fig. 6). Another potential site is the caudal mesopallium (CM),  
98 an auditory forebrain region important to song memory<sup>26,27</sup>. However, blocking DA receptors  
99 in the CM of juvenile males during daily tutoring sessions did not block song copying  
100 (Extended Data Fig. 5i-k).

101 These results show that DA release from PAG axon terminals in HVC (PAG<sub>HVC</sub> terminals)  
102 signals the presence of a suitable model and helps encode this model in the pupil's brain.  
103 Consequently, artificially activating PAG<sub>HVC</sub> terminals should compensate for the absence of a

104 live tutor and facilitate vocal copying in response to song playback. To test this idea, we used  
105 AAVs to express channelrhodopsin-2 (ChR2) bilaterally in the PAG of tutor-naive juvenile  
106 males (Fig. 3i-j, Extended Data Fig. 7a-d). Several weeks ( $33.3 \pm 7.4$  days [mean  $\pm$  SD],  $n =$   
107 6) later, we implanted optical fibers bilaterally over HVC and optogenetically activated  
108 PAG<sub>HVC</sub> terminals while playing an adult male zebra finch song through a speaker. Pairing  
109 PAG<sub>HVC</sub> terminal stimulation with song playback resulted in a significant level of song copying  
110 compared to juveniles that had only been exposed to song playback, or to song playback and  
111 optical illumination of HVC in the absence of ChR2 (Fig. 3j, Extended Data Fig. 7b; see  
112 Methods). Moreover, pairing song playback with PAG<sub>HVC</sub> terminal stimulation while infusing  
113 DA blockers into HVC did not lead to song copying in tutor-naive juveniles (Extended Data  
114 Fig. 7e-g).

115 To explore how tutor-evoked DA release from PAG<sub>HVC</sub> axon terminals alters HVC to drive song  
116 imitation, we implanted tetrodes in the HVC of tutor-naive juveniles and recorded neural  
117 activity before and after their initial encounters with a singing tutor (Fig. 4a-f). Spontaneous  
118 burst firing in HVC neurons increased within 1 h after the juvenile's initial exposure to a  
119 singing tutor (Fig. 4b-c, e), without any change in their mean firing rates (Extended Data Fig.  
120 8d). Because burst firing in HVC is driven by auditory afferents<sup>12</sup>, this enhanced bursting  
121 suggests that tutoring rapidly potentiates auditory inputs to HVC. In fact, brief ( $35.0 \pm 16.8$   
122 min [mean  $\pm$  SD]) experience with a singing tutor led rapidly ( $\sim 1$  h) to the emergence of



123 temporally precise responses in the awake juvenile HVC to tutor song playback (Fig. 4d, f,  
124 Extended Data Fig. 8a-c). Furthermore, the mean firing rate of HVC neurons to song playback  
125 was unaffected by tutoring (Extended Data Fig. 8e-f), indicating that neural responses in HVC  
126 became more tightly locked to specific features in the tutor song. None of these juveniles ( $n =$   
127 4) sang during or for several hours after the tutoring session, and thus these physiological  
128 changes were not simply the result of auditory feedback associated with vocal rehearsal. In  
129 another set of tutor-naive juvenile males, we found that tutoring rapidly reduced the kurtosis  
130 of vocal duration (Fig. 4g-h) and increased the mean entropy variance of the juveniles' songs  
131 (Fig. 4i), two early hallmarks of song copying<sup>7,8</sup>. Notably, blocking DA signaling in the pupil's  
132 HVC with 6-OHDA or DA blockers prevented these physiological and behavioral changes (Fig.  
133 4e, f, h-i).

134 The discovery that DA neurons in the pupil's PAG are strongly and selectively activated by a  
135 singing tutor parallels an emerging body of evidence that potentially homologous neurons in  
136 the mammal can encode social cues, including those related to reward, context, or novelty<sup>16,17</sup>.  
137 Indeed, the present findings advance a model in which both social cues and the song-related  
138 auditory input provided by the singing tutor drive the coincident activation of DA receptors  
139 and auditory synapses in HVC, leading to the rapid emergence of auditory representations of  
140 the tutor's song necessary to song imitation<sup>10,20</sup> (Extended Data Fig. 10). This coincident  
141 encoding mechanism could help ensure that the pupil's brain selectively forms representations

142 of songs produced by suitable adult tutors, and not of extraneous auditory stimuli. Although  
143 DA-dependent modulation of auditory cortical representations has previously been linked to  
144 perceptual learning<sup>28</sup>, a notable feature of the DA-dependent process of auditory encoding  
145 described here is that it occurs in a vocal motor region and rapidly drives vocal imitation. More  
146 broadly, DA signaling is enhanced in the motor cortex of primates relative to other  
147 mammals<sup>29,30</sup>, raising the possibility that augmented DA signaling in motor regions of  
148 songbirds and primates reflects a convergent neural architecture for promoting motor imitation  
149 in response to social models.

150

151 **References**

152

- 153 1 Whiten, A. Social Learning and Culture in Child and Chimpanzee. *Annu Rev Psychol*  
154 **68**, 129-154, doi:10.1146/annurev-psych-010416-044108 (2017).
- 155 2 Goldstein, M. H., King, A. P. & West, M. J. Social interaction shapes babbling:  
156 Testing parallels between birdsong and speech. *Proceedings of the National Academy*  
157 *of Sciences of the United States of America* **100**, 8030-8035,  
158 doi:10.1073/pnas.1332441100 (2003).
- 159 3 Marler, P. & Tamura, M. Culturally Transmitted Patterns of Vocal Behavior in  
160 Sparrows. *Science* **146**, 1483-&, doi:DOI 10.1126/science.146.3650.1483 (1964).
- 161 4 Fehér, O., Wang, H. B., Saar, S., Mitra, P. P. & Tchernichovski, O. De novo  
162 establishment of wild-type song culture in the zebra finch. *Nature* **459**, 564-U594,  
163 doi:10.1038/nature07994 (2009).
- 164 5 Chen, Y., Matheson, L. E. & Sakata, J. T. Mechanisms underlying the social  
165 enhancement of vocal learning in songbirds. *Proceedings of the National Academy of*  
166 *Sciences of the United States of America* **113**, 6641-6646,  
167 doi:10.1073/pnas.1522306113 (2016).
- 168 6 Derégnaucourt, S., Poirier, C., Kant, A. V., Linden, A. V. & Gahr, M. Comparisons of  
169 different methods to train a young zebra finch (*Taeniopygia guttata*) to learn a song. *J*  
170 *Physiol Paris* **107**, 210-218, doi:10.1016/j.jphysparis.2012.08.003 (2013).
- 171 7 Aronov, D., Andalman, A. S. & Fee, M. S. A specialized forebrain circuit for vocal  
172 babbling in the juvenile songbird. *Science* **320**, 630-634,  
173 doi:10.1126/science.1155140 (2008).
- 174 8 Derégnaucourt, S., Mitra, P. P., Feher, O., Pytte, C. & Tchernichovski, O. How sleep  
175 affects the developmental learning of bird song. *Nature* **433**, 710-716,  
176 doi:10.1038/nature03275 (2005).
- 177 9 Nottebohm, F., Stokes, T. M. & Leonard, C. M. Central Control of Song in Canary,  
178 *Serinus-Canarius*. *J Comp Neurol* **165**, 457-486, doi:DOI 10.1002/cne.901650405  
179 (1976).
- 180 10 Roberts, T. F., Gobes, S. M., Murugan, M., Olveczky, B. P. & Mooney, R. Motor  
181 circuits are required to encode a sensory model for imitative learning. *Nat Neurosci*  
182 **15**, 1454-1459, doi:10.1038/nn.3206 (2012).
- 183 11 Fortune, E. S. & Margoliash, D. Parallel Pathways and Convergence onto Hvc and  
184 Adjacent Neostriatum of Adult Zebra Finches (*Taeniopygia-Guttata*). *J Comp Neurol*  
185 **360**, 413-441, doi:DOI 10.1002/cne.903600305 (1995).
- 186 12 Coleman, M. J. & Mooney, R. Synaptic transformations underlying highly selective  
187 auditory representations of learned birdsong. *J Neurosci* **24**, 7251-7265,  
188 doi:10.1523/JNEUROSCI.0947-04.2004 (2004).

- 189 13 Appeltants, D., Absil, P., Balthazart, J. & Ball, G. F. Identification of the origin of  
190 catecholaminergic inputs to HVC in canaries by retrograde tract tracing combined  
191 with tyrosine hydroxylase immunocytochemistry. *J Chem Neuroanat* **18**, 117-133  
192 (2000).
- 193 14 Hamaguchi, K. & Mooney, R. Recurrent interactions between the input and output of  
194 a songbird cortico-basal ganglia pathway are implicated in vocal sequence variability.  
195 *J Neurosci* **32**, 11671-11687, doi:10.1523/JNEUROSCI.1666-12.2012 (2012).
- 196 15 Kingsbury, M. A., Kelly, A. M., Schrock, S. E. & Goodson, J. L. Mammal-like  
197 organization of the avian midbrain central gray and a reappraisal of the intercollicular  
198 nucleus. *PLoS One* **6**, e20720, doi:10.1371/journal.pone.0020720 (2011).
- 199 16 Cho, J. R. *et al.* Dorsal Raphe Dopamine Neurons Modulate Arousal and Promote  
200 Wakefulness by Salient Stimuli. *Neuron* **94**, 1205-1219 e1208,  
201 doi:10.1016/j.neuron.2017.05.020 (2017).
- 202 17 Matthews, G. A. *et al.* Dorsal Raphe Dopamine Neurons Represent the Experience of  
203 Social Isolation. *Cell* **164**, 617-631, doi:10.1016/j.cell.2015.12.040 (2016).
- 204 18 Flores, J. A., Galan-Rodriguez, B., Ramiro-Fuentes, S. & Fernandez-Espejo, E. Role  
205 for dopamine neurons of the rostral linear nucleus and periaqueductal gray in the  
206 rewarding and sensitizing properties of heroin. *Neuropsychopharmacol* **31**, 1475-  
207 1488, doi:10.1038/sj.npp.1300946 (2006).
- 208 19 Sun, F., Zeng, J., Jing, M. Zhou, J., Feng, J., Owen, S. F., Luo, Y., Li, F., Wang, H.,  
209 Yamaguchi, T., Yong, Z., Gao, Y., Peng, W., Wang, L., Zhang, S., Du, J., Lin, D.,  
210 Xu, M., Kreitzer, A. C., Cui, G. & Li, Y. A Genetically Encoded Fluorescent Sensor  
211 Enables Rapid and Specific Detection of Dopamine in Flies, Fish, and Mice. *Cell* **174**,  
212 481-496, doi:10.1016/j.cell.2018.06.042 (2018).
- 213 20 Roberts, T. F., Tschida, K. A., Klein, M. E. & Mooney, R. Rapid spine stabilization  
214 and synaptic enhancement at the onset of behavioural learning. *Nature* **463**, 948-952,  
215 doi:10.1038/nature08759 (2010).
- 216 21 Ungerstedt, U. & Arbuthnott, G. W. Quantitative recording of rotational behavior in  
217 rats after 6-hydroxy-dopamine lesions of the nigrostriatal dopamine system. *Brain Res*  
218 **24**, 485-493 (1970).
- 219 22 Eales, L. A. Song Learning in Zebra Finches - Some Effects of Song Model  
220 Availability on What Is Learnt and When. *Animal Behaviour* **33**, 1293-1300, doi:Doi  
221 10.1016/S0003-3472(85)80189-5 (1985).
- 222 23 Tanaka, M., Singh Alvarado, J., Murugan, M. & Mooney, R. Focal expression of  
223 mutant huntingtin in the songbird basal ganglia disrupts cortico-basal ganglia  
224 networks and vocal sequences. *Proceedings of the National Academy of Sciences of*  
225 *the United States of America* **113**, E1720-1727, doi:10.1073/pnas.1523754113 (2016).

- 226 24 Kubikova, L., Wada, K. & Jarvis, E. D. Dopamine receptors in a songbird brain. *J*  
227 *Comp Neurol* **518**, 741-769, doi:10.1002/cne.22255 (2010).
- 228 25 Hisey, E., Kearney, M. G. & Mooney, R. A common neural circuit mechanism for  
229 internally guided and externally reinforced forms of motor learning. *Nat Neurosci*,  
230 doi:10.1038/s41593-018-0092-6 (2018).
- 231 26 Roberts, T. F. *et al.* Identification of a motor-to-auditory pathway important for vocal  
232 learning. *Nat Neurosci* **20**, 978-986, doi:10.1038/nn.4563 (2017).
- 233 27 London, S. E. & Clayton, D. F. Functional identification of sensory mechanisms  
234 required for developmental song learning. *Nat Neurosci* **11**, 579-586,  
235 doi:10.1038/nn.2103 (2008).
- 236 28 Bao, S., Chan, V. T. & Merzenich, M. M. Cortical remodelling induced by activity of  
237 ventral tegmental dopamine neurons. *Nature* **412**, 79-83, doi:10.1038/35083586  
238 (2001).
- 239 29 Berger, B., Gaspar, P. & Verney, C. Dopaminergic innervation of the cerebral cortex:  
240 unexpected differences between rodents and primates. *Trends Neurosci* **14**, 21-27  
241 (1991).
- 242 30 Williams, S. M. & Goldman-Rakic, P. S. Widespread origin of the primate  
243 mesofrontal dopamine system. *Cereb Cortex* **8**, 321-345 (1998).
- 244

## 245 **Acknowledgements**

246 We thank Jordan Hatfield for constructing AAV2/9-CAG-GRAB<sub>DA1h</sub>. We also thank Stephen  
247 Nowicki, Susan Peters, Christopher Sturdy, Fan Wang, and Scott Soderling for critical  
248 discussion and for reading earlier versions of this manuscript. This work was supported by  
249 JSPS Postdoctoral Fellowship for Research Abroad (M.T.), the National Basic Research  
250 Program of China 973 Program Grant 2015CB856402 (Y.L.), the American BRAIN Initiative  
251 project 1U01NS103558-01 (Y.L.), NIH Grant 1R01-NS-099288 (R.M.), and NSF IOS-  
252 1354962 (R.M.).

## 253 **Author contributions**

254 M.T. and R.M. designed experiments. F.S. and Y.L. developed DA sensors, M.T. performed  
255 experiments and analyzed data. M.T. and R.M. wrote the manuscript.

256 **Data availability**

257 The datasets generated and analyzed during the current study are available from the  
258 corresponding author on reasonable request.

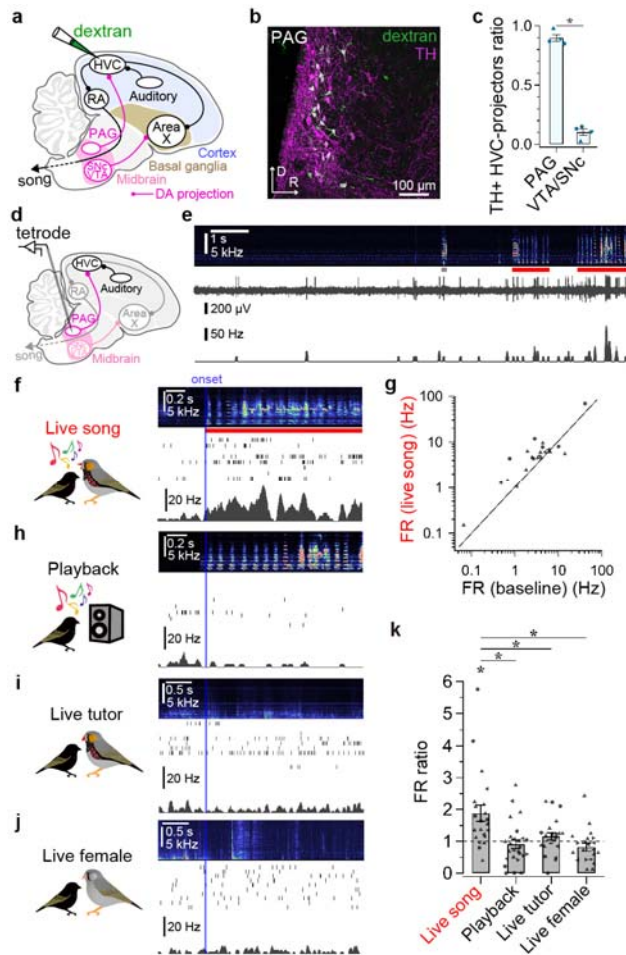
259 **Competing interests**

260 F.S. and Y.L. have filed patent applications whose value might be affected by this publication.

261 **Correspondence and requests for materials** should be addressed to R.M.

262

263 **Figure legends**

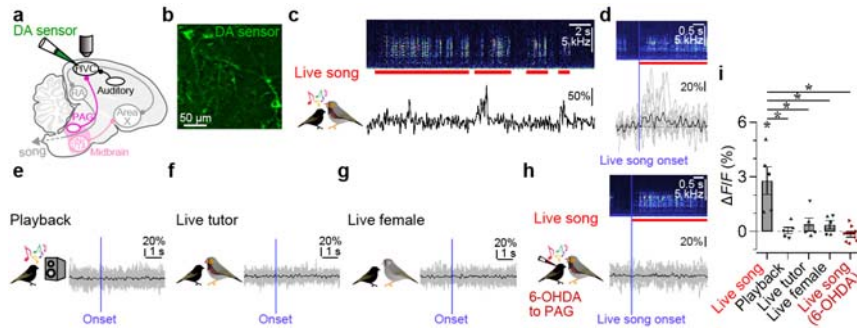


264

265 **Figure 1 | Recordings of PAG activity.**

266 **a**, Schematics of dextran injection into HVC. **b**, PAG neurons labeled with dextran (green) and  
 267 TH antibody (pseudo-colored magenta) (~0.5 mm lateral, R: rostral, V: ventral). **c**, Proportion  
 268 of double-labeled neurons (dextran and TH) in the midbrain ( $\chi^2$ -test:  $\chi^2(1) = 623.02$ ,  $P < 0.001$ ,  
 269  $n = 4$  hemispheres from 3 birds). **d**, Schematics of tetrode recordings from PAG neurons. **e**,  
 270 PAG unit activity during live tutor songs (red bar) (gray bar: an isolated tutor call) (top: sound  
 271 spectrogram, middle: voltage recording, bottom: firing rate). **f**, PAG unit activity aligned to the  
 272 onset of tutor songs (top: averaged spectrogram, middle: spike raster, bottom: mean firing rate).  
 273 **g**, Mean firing rate (FR) during live tutor songs as a function of baseline FR of PAG neurons.  
 274 **h-j**, PAG unit activity aligned to the onset of song playback (**h**), encounters with a live, non-  
 275 singing tutor (**i**), encounters with a live female (**j**), shown as in **f**. **k**, Mean FR of PAG neurons  
 276 normalized to baseline FR (two-sided paired  $t$ -test: Live song:  $t(21) = 3.439$ ,  $P = 0.002$ ;  
 277 Playback:  $t(25) = 0.278$ ,  $P = 0.783$ ; Live tutor:  $t(21) = 1.270$ ,  $P = 0.218$ ; Live female:  $t(19) =$   
 278  $1.339$ ,  $P = 0.196$ ;  $n = 26$  neurons, 5 birds). Error bars indicate mean  $\pm$  SEM.

279

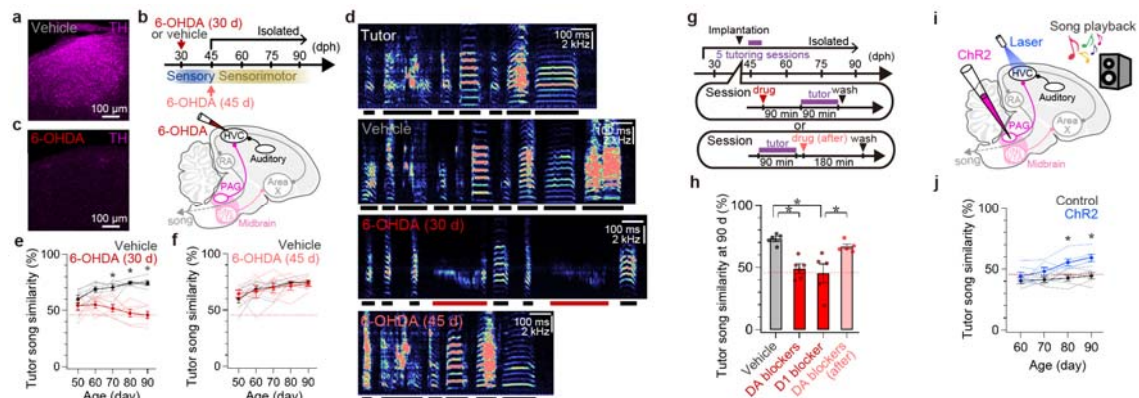


280

281 **Figure 2 | Imaging of DA in HVC.**

282 **a**, Schematics of two-photon imaging of DA sensors (GRAB<sub>DA1h</sub>) in HVC. **b**, Two-photon  
 283 image of HVC neurons expressing DA sensors. **c**, Fluorescence changes ( $\Delta F/F$ ) of GRAB<sub>DA1h</sub>  
 284 in a juvenile's HVC neuron in response to live tutor songs (red bars) **d**,  $\Delta F/F$  aligned to the  
 285 onset of live tutor songs (gray: individual, black: mean). **e-h**,  $\Delta F/F$  aligned to the onset of song  
 286 playback (**e**), encounters with a live, non-singing tutor (**f**), encounters with a live female (**g**),  
 287 and live tutor songs after 6-OHDA injection into PAG (**h**). **i**, Mean  $\Delta F/F$  of HVC neurons (two-  
 288 sided paired *t*-test: Live song:  $t(4) = 3.660$ ,  $P = 0.022$ ; Playback:  $t(4) = 0.261$ ,  $P = 0.807$ ; Live  
 289 tutor:  $t(4) = 1.092$ ,  $P = 0.336$ ; Live female:  $t(4) = 1.589$ ,  $P = 0.187$ ; Live song after 6-OHDA  
 290 injection into PAG:  $t(7) = 1.122$ ,  $P = 0.324$ ;  $n = 13$  neurons, 5 birds). Error bars indicate mean  
 291  $\pm$  SEM.

292



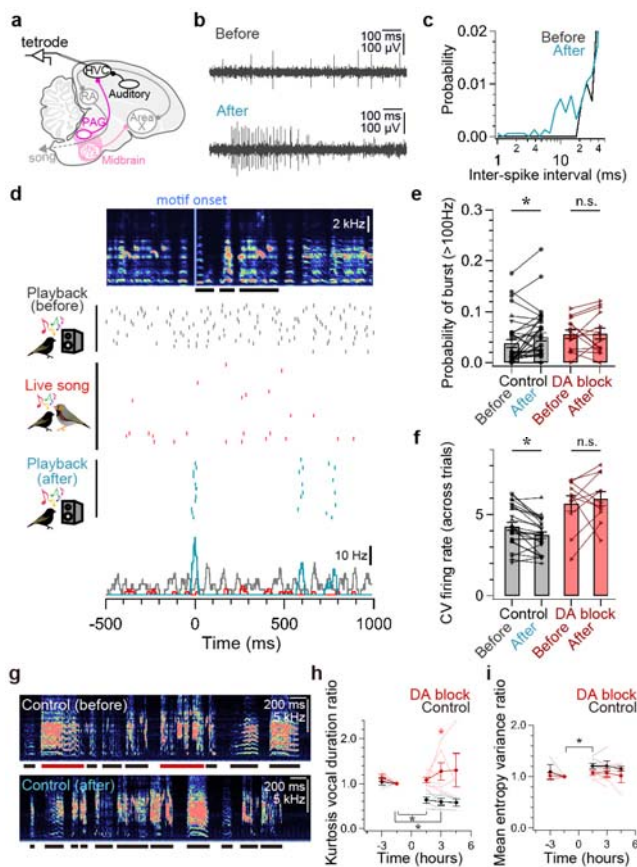
293

294 **Figure 3 | Chemical blockade and optogenetic activation of DA signaling in HVC.**

295 **a**, DA fibers in HVC (pseudo-colored magenta: TH) (~2.4 mm lateral). **b**, Timeline and  
 296 schematics of 6-OHDA injection into HVC. **c**, Loss of DA fibers in HVC after 6-OHDA  
 297 injection at 29 d, as in **a** (~2.4 mm lateral). **d**, From top to bottom, spectrograms of a song from  
 298 the tutor bird and songs from 90-d pupil birds that received injection into HVC of vehicle, 6-  
 299 OHDA at ~30 d, or 6-OHDA at ~45 d (red bars denote abnormally long syllables. See Extended  
 300 Data Fig. 4b-c). **e**, Absence of song copying following injection of 6-OHDA into HVC at ~30  
 301 d (Tukey-Kramer test: vehicle:  $n = 7$ , 6-OHDA:  $n = 7$ ; at 90 d:  $P < 0.001$ ). **f**, Normal levels of  
 302 song copying were achieved following injection of 6-OHDA into HVC at ~45 d (Tukey-Kramer



303 test: vehicle:  $n = 7$  [same birds as in **e**], 6-OHDA at 45 d:  $n = 6$ ; at 90 d:  $P = 1.000$ ). **g**, Timeline  
 304 of DA blocker infusion into HVC using microdialysis. **h**, Tutor song similarity of 90-d pupils  
 305 that received infusion into HVC of vehicle during tutoring ( $n = 5$ ), DA blockers during tutoring  
 306 (Tukey-Kramer test: vs. vehicle:  $P = 0.011$ ,  $n = 5$ ), D1-type blocker during tutoring (Tukey-  
 307 Kramer test: vs. vehicle:  $P < 0.001$ ,  $n = 5$ ), or DA blockers after tutoring (Tukey-Kramer test:  
 308 vs. vehicle:  $P = 1.000$ ;  $n = 5$ ). **i**, Schematics of  $PAG_{HVC}$  terminal activation paired with song  
 309 playback. **j**, Song copying is facilitated by pairing playback with  $PAG_{HVC}$  terminal activation  
 310 in tutor-naive juveniles (Tukey-Kramer test: Chr2:  $n = 6$ ; control:  $n = 6$ ; at 90 d:  $P = 0.023$ ).  
 311 Horizontal red dashed lines in **e**, **f**, **h**, and **j** show song similarity between 90-d untutored birds  
 312 to unrelated adults (See Extended Data Fig. 4b-c). Error bars indicate mean  $\pm$  SEM.  
 313



314

315 **Figure 4 | Changes in HVC activity and song features after live tutoring.**

316 **a**, Schematic of HVC recordings in pupils. **b-c**, Spontaneous HVC unit activity (**b**) and the  
 317 histogram of the interspike intervals before (black) and after (cyan) live tutoring (**c**). **d**, HVC  
 318 unit activity aligned to tutor song motif onset (top: averaged spectrogram; middle: raster,  
 319 bottom: mean FR across trials; horizontal bars: syllables). **e**, Probability of burst activity (>100  
 320 Hz) increased after live tutoring in control juveniles (two-sided paired  $t$ -test:  $t(34) = 2.490$ ,  $P$   
 321 = 0.018,  $n = 35$  neurons, 4 birds), but not in juveniles with 6-OHDA injected into HVC (two-

322 sided paired  $t$ -test:  $t(13) = 0.774$ ,  $P = 0.453$ ,  $n = 14$  neurons, 2 birds). **f**, Coefficients of variance  
323 (CV) of firing rate across trials increased in control juveniles (two-sided paired  $t$ -test:  $t(25) =$   
324  $4.080$ ,  $P < 0.001$ ,  $n = 26$  neurons, 4 birds), but not in juveniles with 6-OHDA injected into  
325 HVC (two-sided paired  $t$ -test:  $t(10) = 0.640$ ,  $P = 0.537$ ,  $n = 11$  neurons, 2 birds). **g**,  
326 Spectrograms of juvenile songs before (top) and after (bottom) live tutoring (red bar: long  
327 vocalization). **h**, After live tutoring, kurtosis of vocal duration decreased in control juveniles  
328 (two-sided paired  $t$ -test: 1.5 h:  $t(5) = 5.563$ , Bonferroni corrected  $P = 0.008$ ,  $n = 6$ ), but not in  
329 juveniles with 6-OHDA or DA blockers injected into HVC (two-sided paired  $t$ -test: 1.5 h:  $t(5)$   
330  $= 1.364$ , Bonferroni corrected  $P = 0.692$ ,  $n = 6$ ). **i**, After live tutoring, mean Wiener entropy  
331 variance (EV) increased in control juveniles (two-sided paired  $t$ -test: at 1.5 h:  $t(5) = 4.059$ ,  
332 Bonferroni corrected  $P = 0.029$ ,  $n = 6$ ), but not in juveniles with 6-OHDA or DA blockers  
333 injected into HVC (two-sided paired  $t$ -test: at 1.5 h:  $t(5) = 1.432$ , Bonferroni corrected  $P =$   
334  $0.635$ ,  $n = 6$ ). Juveniles did not sing during tutoring (0-1.5 h. See Extended Data Fig. 9). Error  
335 bars indicate mean  $\pm$  SEM.  
336

337 **Methods**

338 **Animal model**

339 Juvenile male (15-90 d), adult male (>200 d), and adult female (>200 d) zebra finches  
340 (*Taeniopygia guttata*) were obtained from the Duke University Medical Center breeding  
341 facility. All experimental procedures were in accordance with the NIH guidelines and approved  
342 by the Duke University Medical Center Animal Care and Use Committee. Birds were kept  
343 under a 14/10-h light/dark cycle with free access to food and water. Data were collected from  
344 96 birds (Supplementary Table).

345 **Song analysis**

346 Songs were automatically recorded with Sound Analysis Pro (SAP2011)<sup>31</sup> in a soundproof box.  
347 Vocalizations of >10 ms were detected by thresholding of the recorded sounds. Imitation of the  
348 tutor song was quantified as percent similarity (asymmetrical similarity) between the song  
349 motifs from pupil birds and their tutors using SAP2011<sup>31</sup> with default parameters for zebra  
350 finches, and reported as tutor song similarity. First, the song motif (a stereotyped sequence of  
351 syllables constituting an adult zebra finch song) of each bird was determined as the most  
352 frequently observed syllable sequence. Then, percent similarity was calculated for  
353 representative song motifs randomly chosen from pupils and their tutor, and averaged across  
354  $\geq 10$  comparisons to report as tutor song similarity. For immature subsongs that do not have a  
355 stereotyped song motif, we used randomly chosen part of subsongs with the duration similar to  
356 the tutor song motif for calculating percent similarity. For isolated birds in Extended Data Fig.  
357 4c, percent similarity was calculated between the song motifs from isolated birds and unrelated,  
358 normally raised adult zebra finches. A song bout was detected as successive vocalizations with  
359  $\geq 3$  syllables (to exclude call bouts) separated by an inter-bout interval of >400 ms. Kurtosis of  
360 vocal duration and Wiener entropy variance (EV) were calculated based on all the song bouts  
361 in each 90-minute time window.

362 **Tutoring of juvenile birds**

363 Juvenile birds were raised by their parents with their siblings until ~45 d in experiments  
364 depicted in Fig. 3a-f. Otherwise, juvenile birds were separated from their parents and siblings  
365 at 15-30 d (i.e., tutor-naive juveniles), and encountered an unfamiliar adult male (tutor) only  
366 during tutoring sessions. During a tutoring session, a juvenile bird and tutor were separated by  
367 a plastic grating or transparent glass, so they could acoustically and visually interact but direct  
368 physical interactions were prevented. The tutor was either manually introduced into the  
369 neighboring chamber by an experimenter, or presented through an electric glass whose  
370 transparency can be remotely controlled. Attention of juvenile birds to the tutor was quantified  
371 as the time that juvenile birds were awake and near the tutor without foraging, drinking,  
372 preening, or singing, and normalized to the total time of observation (>5 min) during tutoring

373 sessions. Untutored isolated birds depicted in Extended Data Fig. 4b-c were kept isolated from  
374 adult males until 90 d.

### 375 **General surgery**

376 Detailed procedures of surgery were previously provided<sup>23</sup>. Briefly, juvenile birds were  
377 anesthetized with 2% isoflurane inhalation and placed on a custom stereotaxic apparatus with  
378 a heat blanket. Target cites for injection and implantation were determined by stereotaxic  
379 coordinates and multiunit activity. Stereotaxic coordinates were [0.0 mm rostral, 2.4 mm  
380 lateral, and 0.5 mm ventral] for HVC; [3.4 mm rostral, 0.5 mm lateral, and 6.3 mm ventral  
381 (head angle: 58°)] for PAG; [5.8 mm rostral, 1.6 mm lateral, and 3.0 mm ventral (head angle:  
382 40°)] for Area X; and [1.3 mm rostral, 1.2 mm lateral, and 0.5 mm ventral] for CM. Reagents  
383 or viruses were injected using Nanoject-II (Drummond Scientific). Viral injection was  
384 performed bilaterally with the volume of 483-966 nL per hemisphere. Viruses were obtained  
385 from the Penn Vector Core (Pennsylvania, USA), UNC Vector Core (Chapel Hill, USA),  
386 Janelia Virus Service Facility (Ashburn, USA), and Vigene Biosciences (Rockville, USA).  
387 Experiments were performed >30 d after the viral injection. Birds with unsuccessful injection  
388 or implantation were discarded from the analysis.

### 389 **Injection of 6-OHDA**

390 Juvenile birds received bilateral injection of 200-450 nL 6-OHDA solution into HVC at either  
391 ~30 d (mean ± SD: 30.1 ± 4.2 d, range: 25-34 d,  $n = 7$ ) or ~45 d (mean ± SD: 44.5 ± 3.0 d,  
392 range: 39-47 d,  $n = 6$ ). The solution was PBS-based and included 5-20 mM 6-OHDA  
393 hydrochloride (Santa Cruz, sc-203482), 10 mM L-ascorbic acid (MilliporeSigma, A92902),  
394 and 1 μM desipramine hydrochloride (Tocris, 3067), which was included as an inhibitor for  
395 noradrenaline and serotonin transporters to protect noradrenergic and serotonergic neurons at  
396 the injection site. Control birds received injection of PBS with 10 mM ascorbic acid and 1 μM  
397 desipramine at ~30 d (mean ± SD: 29.3 ± 3.6 d, range: 22-32 d,  $n = 7$ ). Drugs were dissolved  
398 into PBS immediately before injection in place of equimolar NaCl (Working solution: ~300  
399 mOsm, pH 7.3). After injection, birds were returned to their original home cage until ~45 d  
400 when they were isolated in a soundproof box until 90 d.

### 401 **Microdialysis infusion of drugs**

402 Tutor-naive juveniles (~45 d, mean ± SD: 43.8 ± 5.5 d, range: 32-57 d,  $n = 34$ ) received bilateral  
403 implantation of a microdialysis probe. After 1-3 d of implantation (mean ± SD: 45.5 ± 5.8 d,  
404 range: 33-60 d,  $n = 34$ ), tutoring sessions were conducted for 5 consecutive days. Each tutoring  
405 session consisted of 90-minute tutor presentation. Drug was infused into the target area (HVC,  
406 Area X, CM, or PAG) either 90 minutes before or immediately after the tutor presentation, and  
407 washed with saline 180 minutes after the injection (Fig. 3g). The tutor bird typically sang >30  
408 motifs in a session (See Extended Data Fig. 5e). For a session in which the tutor did not sing  
409 any song, an additional tutoring session was conducted on the next day. As a blocker for D1-  
410 and D2-type receptors, 5 mM R(+)-SCH-23390 hydrochloride (MilliporeSigma, D054) and 5

411 mM S(-)-sulpiride (Tocris, 0895) were respectively used and dissolved into saline. To  
412 inactivate PAG, 2.5 mM muscimol (MilliporeSigma, M-1523) dissolved into saline was infused  
413 into the PAG.

#### 414 **Histology and imaging**

415 Birds were deeply anesthetized with intramuscular injection of 20  $\mu$ L Euthasol (Virbac) and  
416 transcardially perfused with PBS, followed by perfusion with 4% (wt/vol) paraformaldehyde  
417 (PFA) in PBS. The removed brain was post-fixed and cryoprotected with 30% (wt/vol) sucrose  
418 and 4% (wt/vol) PFA in PBS overnight. Frozen sagittal sections (thickness of 50  $\mu$ m) were  
419 prepared with a sledge microtome (Reichert) and collected in PBS. For immunohistochemistry,  
420 sections were washed twice in PBS, permeabilized with 0.3% Triton X-100 in PBS (PBST) for  
421 1 h, blocked with 10% Blocking One Histo (06349-64, Nacalai Tesque) in PBST for 1 h, and  
422 incubated with rabbit primary antibody for TH (1:500, AB152; MilliporeSigma) or rabbit  
423 primary antibody for DBH (1:2000, #22806; ImmunoStar) in PBST with 10% Blocking One  
424 Histo at 4  $^{\circ}$ C overnight. Then, sections were washed three times in PBST and incubated with  
425 anti-rabbit secondary antibody (1:500; Jackson ImmunoResearch) in PBST at room  
426 temperature for 1 h, followed by three washes in PBS. Sections were coverslipped with  
427 Fluoromount-G (SouthernBiotech), and then imaged with a confocal microscope (SP8; Leica)  
428 through a 20x objective lens controlled by LAS X software (Leica). To label PAG neurons that  
429 project to HVC or Area X, dextran Alexa Fluor 488 (D-22910; ThermoFisher) was injected  
430 into HVC or Area X of juvenile birds (Age: mean  $\pm$  SD: 35.3  $\pm$  7.0 d, range: 28-42 d,  $n$  = 3 for  
431 HVC, Age: mean  $\pm$  SD: 47.7  $\pm$  15.3 d, range: 36-65 d,  $n$  = 3 for Area X) 4–7 d before perfusion.  
432 Retrogradely labeled neurons were manually counted in PAG and SNc/VTA, each of which  
433 was densely packed with TH-positive (TH+) neurons. Images were shown as max-projected  
434 images of sagittal sections. To quantify TH+ fibers in HVC, TH+ fibers in HVC shelf/NCL,  
435 and DBH+ fibers in HVC, the fiber density was calculated in  $>0.04$  mm<sup>2</sup> areas from each region  
436 as the fraction of areas with the fluorescence more than [mean + 10 SD] of the background  
437 fluorescence. For analysis on HVC shelf/NCL, a  $>0.04$  mm<sup>2</sup> region located  $\sim$ 0.6 mm ventral  
438 from HVC was manually selected.

#### 439 **Two-photon imaging and analysis**

440 Viruses coding DA sensors (AAV2/9-hSyn-GRAB<sub>DA1h</sub> or AAV2/9-CAG-GRAB<sub>DA1h</sub>),  
441 developed in Yulong Li's lab<sup>19</sup>, were injected into HVC of tutor-naive juveniles ( $\sim$ 30 d, mean  
442  $\pm$  SD: 32.6  $\pm$  5.3 d, range: 25-39 d,  $n$  = 5), and HVC was imaged after implantation of a head-  
443 post and cranial window  $>30$  days later (mean  $\pm$  SD: 66.6  $\pm$  6.0 d, range: 60-73 d,  $n$  = 5). To  
444 ablate DA-releasing PAG neurons, 200 nL 6-OHDA solution (10 mM 6-OHDA, 10 mM L-  
445 ascorbic acid, and 1  $\mu$ M desipramine hydrochloride) was injected into PAG 2 days before  
446 imaging. Images were collected at 15.5 Hz with a resonant scanning two-photon microscope  
447 (NeuroLabware) that applies a mode-locked titanium sapphire laser (Mai Tai DeepSee) at 920  
448 nm through a 16x objective lens (0.8 NA water immersion, Nikon). The objective lens was

449 covered with black cloth to prevent room light from being detected by the photomultipliers.  
450 During imaging, a head-fixed bird in a dim room experienced playback of an adult zebra finch  
451 (tutor) song bout (3 seconds. 7 introductory notes and 3 motifs comprising 5 syllables),  
452 encounters with an adult male tutor, encounters with an adult female bird, and a singing tutor  
453 with a randomized order. Images were acquired >10 trials for each condition, and regions of  
454 interest (ROIs) were automatically or manually selected after image alignment with MATLAB  
455 programs (Scanbox). After subtraction of background fluorescence in an annular region  
456 surrounding each ROI, signals were calculated as mean fluorescence within each ROI. Then,  
457  $\Delta F/F$  of the ROI was calculated for each trial as  $100 * (F(t) - F_0) / F_0$  [%], where  $F(t)$  was a  
458 time series of ROI signals, and  $F_0$  was the average of baseline ROI signals for the 5 s-period  
459 just before the onset of stimulus presentation. Mean  $\Delta F/F$  was calculated for the 5 s-period  
460 after the onset of stimulus presentation, and averaged across trials in each condition.

### 461 **Optogenetics**

462 Tutor-naive juvenile birds received injection of either AAV2/9-CAG-ChR2-mCherry, AAV2/1-  
463 CAG-ChR2-mCherry, or AAV2/9-CAG-NRX-ChR2-YFP to PAG at ~35 d (mean  $\pm$  SD: 34.0  
464  $\pm$  4.8 d, range: 30-40 d,  $n = 9$ ). Laser was bilaterally applied through optic fibers (core: 200  
465  $\mu$ m; Thorlabs) implanted to HVC. Juvenile birds received a tutoring session per day for 5  
466 consecutive days starting at ~60-70 d (mean  $\pm$  SD: 64.0  $\pm$  4.9 d, range: 61-71 d,  $n = 9$ ). In each  
467 tutoring session, a juvenile bird experienced playback of a song bout (mean amplitude: 70 dB  
468 SPL, 7 introductory notes and 3 motifs comprising 5 syllables) 10 times (30 motifs) within 30  
469 minutes. To block DA signaling in HVC, DA blockers were infused into HVC with  
470 microdialysis probes 90 minutes before the tutoring session, and washed with saline  
471 immediately after the tutoring session ( $n = 3$ ). Experimental birds received repetitive laser  
472 stimulation (10 ms; 20 Hz) throughout the playback. Control birds consisted of a group that  
473 received injection of viruses coding GFP and implantation of optic fibers ( $n = 2$ , scAAV2/9-  
474 CMV-GFP or AAV2/9-CAG-GFP) at ~35 d (mean  $\pm$  SD: 36.5  $\pm$  6.4 d, range: 32-41 d,  $n = 2$ ),  
475 a group that did not receive viral injection but implantation of optic fibers ( $n = 2$ ), and a group  
476 that did not receive injection, implantation, or laser stimulation ( $n = 2$ ). These groups listened  
477 to playback in the same way as experimental birds (Age: mean  $\pm$  SD: 58.5  $\pm$  8.5 d, range: 54-  
478 73 d,  $n = 6$ ), and were analyzed together since we did not find significant differences in learning  
479 abilities between these groups.

### 480 **Chronic recording from PAG and HVC**

481 Tetrodes (A2x2-tet-3/10mm-150-150-121, NeuroNexus) were implanted into the HVC or the  
482 PAG of tutor-naive juveniles (Age: mean  $\pm$  SD: 51.3  $\pm$  13.4 d, range: 27-71 d,  $n = 11$ ). Birds  
483 were habituated to a dummy probe (1.5-2 g) on the head for ~7 d before the implantation. Data  
484 were collected with a universal serial bus (USB) interface board (RHD2000; Intan  
485 Technologies) after band-pass filtering (0.2–10 kHz) and sampling at 30 kHz with a small  
486 amplifier board (RHD2132 16-Channel; Intan Technologies) on the bird's head. Unit activity

487 was sorted in a semi-automated fashion with a custom C++ software using a support vector  
488 machine algorithm (M.T.). Unit activity with a mean amplitude  $>3$  SD of noise was used for  
489 subsequent analysis. Recording of song-related activity was triggered by `xpctarget` in  
490 MATLAB (MathWorks). To block DA signaling in HVC, juvenile birds received an injection  
491 of 6-OHDA into HVC 2-5 days before tetrode recording from the same HVC. Mean FR of PAG  
492 neurons was calculated for  $>10$  trials with  $>0.5$  seconds after the onset of singing or song  
493 playback and 5 s after presentation of a male or female bird, and averaged after normalization  
494 with mean spontaneous FR calculated for  $>10$  seconds before the presentation of stimuli.  
495 Probability of burst activity in HVC neurons was calculated for  $>300$  s spontaneous activity  
496 before and after exposure to a live tutor. CV FR across trials of HVC neurons was calculated  
497 for 50 ms-bin with a hop size 1 ms across  $>15$  trials, and reported as average of CV FR from  
498 all the bins in the motif ( $>0.5$  seconds) if the mean FR during playback was  $>0.05$  Hz. For data  
499 analysis, Igor Pro (WaveMetrics), MATLAB, and Microsoft Excel were used.

## 500 **Statistics**

501 Error bars and values in the text indicate mean  $\pm$  standard error of mean (SEM), unless  
502 otherwise noted. Two-way ANOVA was performed in MATLAB to examine significance of  
503 the main effect of 6-OHDA ( $F(2,85) = 53.10, P < 0.001$ ) (Fig. 3e-f), DA blockers to HVC, DA  
504 blockers to CM, and muscimol to PAG ( $F(5,99) = 23.17, P < 0.001$ ) (Fig. 3h and Extended  
505 Data Fig. 5c, h, k), DA blockers to Area X ( $F(1,30) = 0.22, P = 0.640$ ) (Extended Data Fig. 6c),  
506 optogenetic activation of PAG terminals in HVC ( $F(2,47) = 16.61, P < 0.001$ ) (Fig. 3j and  
507 Extended Data Fig. 7f), followed by post-hoc Tukey-Kramer test to report significant  
508 difference between conditions at each age window. To examine the different proportion of  
509 labeled neurons in PAG and VTA/SNc,  $\chi^2$ -tests were performed. Two-way ANOVA was  
510 performed in MATLAB to examine significance of the main effect of blockage of DA signaling  
511 on kurtosis syllable duration ( $F(1,39) = 19.69, P < 0.001$ ) (Fig. 4h), entropy variance ( $F(1,39)$   
512  $= 4.84, P = 0.034$ ) (Fig. 4i), and song rate ( $F(1,39) = 0.16, P = 0.691$ ) (Extended Data Fig. 9),  
513 followed by Tukey-Kramer test to report significant difference between conditions at each time  
514 window, and by paired  $t$ -test with Bonferroni correction to report significant difference between  
515 before and after exposure to tutor songs. One-way ANOVA was performed in MATLAB to  
516 examine the main effect of different conditions in Fig. 1k and Extended Data Fig. 2b ( $F(4,93)$   
517  $= 6.84, P < 0.001$ ), Fig. 2i ( $F(4,23) = 10.31, P < 0.001$ ), Extended Data Fig. 3c ( $F(2,12) =$   
518  $13.42, P < 0.001$ ), Extended Data Fig. 3d ( $F(2,12) = 0.14, P = 0.870$ ), Extended Data Fig. 4a  
519 ( $F(2,17) = 0.28, P = 0.757$ ), Extended Data Fig. 5d ( $F(2,7) = 30.40, P < 0.001$ ), and Extended  
520 Data Fig. 5e ( $F(2,10) = 0.78, P = 0.486$ ), each followed by Tukey-Kramer test to report  
521 significant difference between conditions. In other analyses, paired  $t$ -test (Figs. 1k, 2i, 4h,i,  
522 Extended Data Figs. 2b, 8d-f) or unpaired  $t$ -tests (Extended Data Figs. 3e, 4c) were performed  
523 in Microsoft Excel. Multiple data from a bird are indicated with the same markers in Figs.  
524 1c,g,k, 2i, 4e,f and Extended Data Figs. 1b,c,e,f,g, 2b, 3c-e, 8d-f. Statistical tests performed

525 were two-sided. Asterisks show  $P < 0.050$ .

526 **Code availability**

527 Custom code or software is available from the corresponding author upon reasonable request.

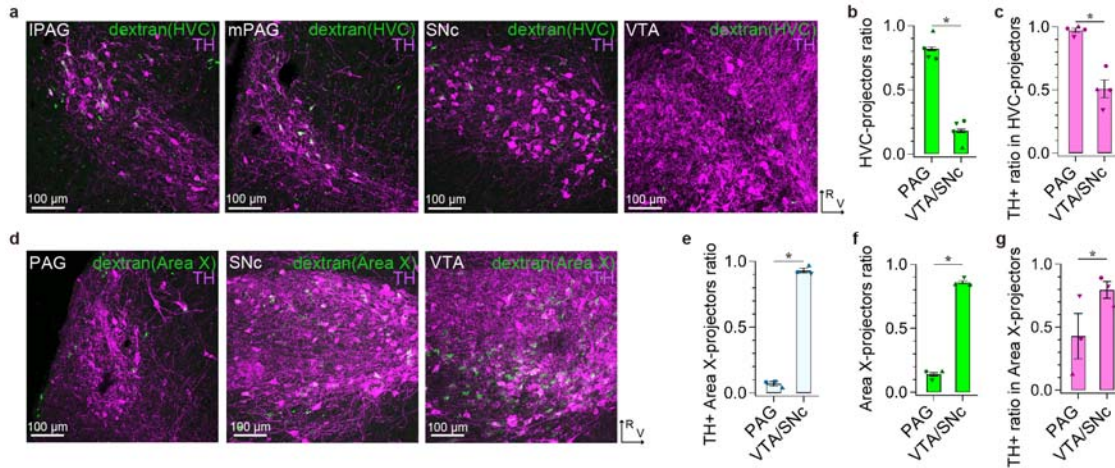
528 **Method references**

529 31 Tchernichovski, O., Nottebohm, F., Ho, C. E., Pesaran, B. & Mitra, P. P. A procedure  
530 for an automated measurement of song similarity. *Anim Behav* **59**, 1167-1176,  
531 doi:10.1006/anbe.1999.1416 (2000).

532



533 **Extended Data figure legends**

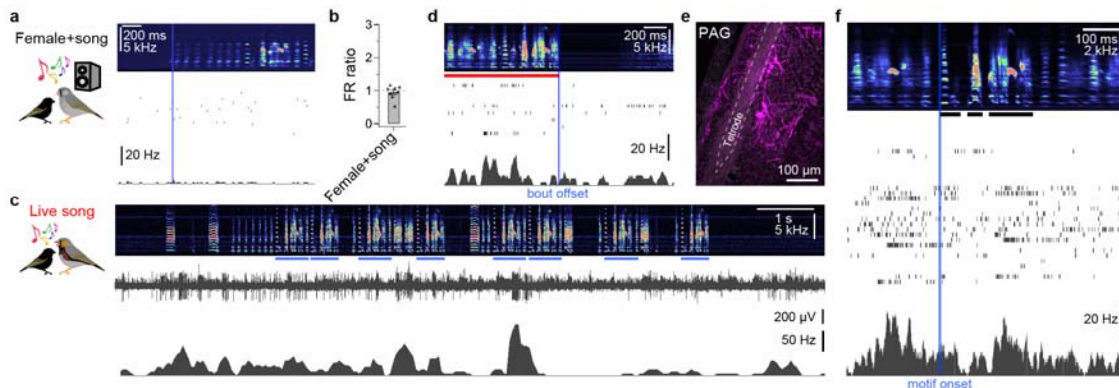


534

535 **Extended Data Figure 1 | Distribution of HVC-projecting neurons and Area X-projecting**  
 536 **neurons in the midbrain.**

537 **a**, From left to right, a max-projected image of serial sagittal sections visualized with a confocal  
 538 microscope, showing a lateral part of PAG (IPAG) (~1.0 mm lateral), a medial part of PAG  
 539 (mPAG, ~0.2 mm lateral), SNc (~1.2 mm lateral), and VTA (~0.2 mm lateral), each of which  
 540 was labeled with dextran injected into HVC (green) and an antibody for TH (pseudo-colored  
 541 magenta). Similar results were obtained in 4 independently repeated experiments (R: rostral,  
 542 V: ventral). **b**, Proportion of HVC-projecting neurons in PAG and VTA/SNc ( $\chi^2$ -test:  $\chi^2(1) =$   
 543  $406.54$ ,  $P < 0.001$ ,  $n = 4$  hemispheres from 3 birds). **c**, Proportion of TH-positive (TH+)  
 544 neurons in HVC-projecting neuron subsets in PAG and VTA/SNc ( $\chi^2$ -test:  $\chi^2(1) = 204.62$ ,  $P <$   
 545  $0.001$ ,  $n = 4$  hemispheres from 3 birds). **d**, From left to right, a max-projected image of serial  
 546 sagittal sections visualized with a confocal microscope, showing PAG (~0.6 mm lateral), SNc  
 547 (~0.6 mm lateral), and VTA (~0.2 mm lateral), each of which was labeled with dextran injected  
 548 into Area X (green) and an antibody for TH (pseudo-colored magenta). Similar results were  
 549 obtained in 3 independently repeated experiments. **e**, Proportion of double-labeled neurons  
 550 (dextran and TH) in PAG and SNc/VTA ( $\chi^2$ -test:  $\chi^2(1) = 493.92$ ,  $P < 0.001$ ,  $n = 3$  hemispheres  
 551 from 3 birds) in birds that received injection of dextran into Area X. **f**, Proportion of Area X-  
 552 projecting neurons in PAG and VTA/SNc ( $\chi^2$ -test:  $\chi^2(1) = 472.07$ ,  $P < 0.001$ ,  $n = 3$  hemispheres  
 553 from 3 birds). **g**, Proportion of TH+ neurons in Area X-projecting neuron subsets in PAG and  
 554 VTA/SNc ( $\chi^2$ -test:  $\chi^2(1) = 55.14$ ,  $P < 0.001$ ,  $n = 3$  hemispheres from 3 birds). Error bars indicate  
 555 mean  $\pm$  SEM.

556

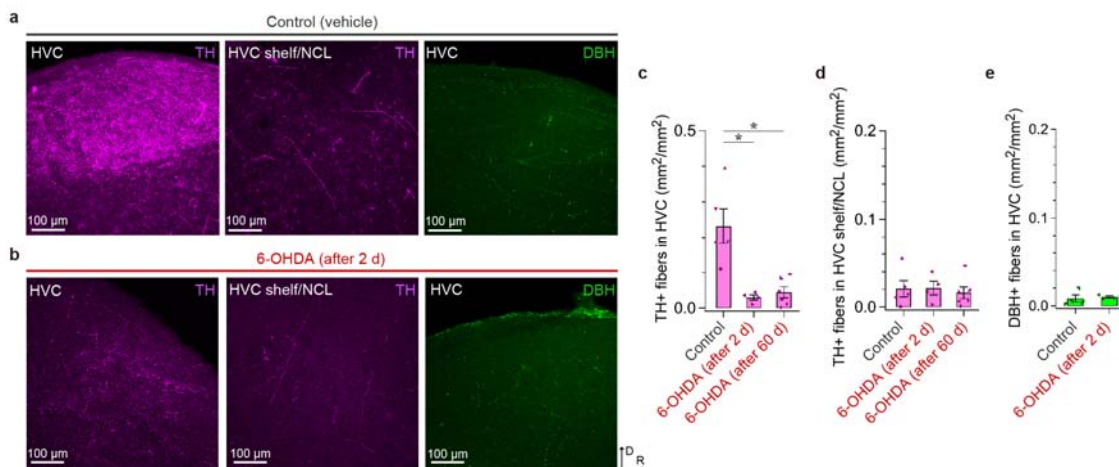


557

558 **Extended Data Figure 2 | Juvenile male PAG activity in response to song playback in the**  
 559 **presence of a female bird and live songs of a male bird.**

560 **a**, Tutor-naive juvenile male finch PAG activity aligned to the onset of 35 presentations of song  
 561 playback in the presence of an adult female bird (top: averaged sound spectrogram, middle:  
 562 spike raster plot, bottom: mean firing rate). **b**, Mean firing rate (FR) during presentation of  
 563 song playback in the presence of a female bird, normalized to baseline FR (two-sided paired *t*-  
 564 test:  $t(7) = 0.620$ ,  $P = 0.555$ ;  $n = 8$  neurons from 2 birds). **c**, PAG activity during a tutor song  
 565 bout (top: sound spectrogram, middle: voltage recording, bottom: firing rate, blue bar: song  
 566 motif). **d**, PAG unit activity aligned to the offset of a live tutor's song bouts (red bar: live song),  
 567 shown as in **a**. **e**, A max-projected image of serial sagittal sections visualized with a confocal  
 568 microscope, showing the site of tetrode recordings in PAG (~0.8 mm lateral of the midline). **f**,  
 569 PAG unit activity aligned to the onset of live tutor's song motifs, shown as in **a**. Note that the  
 570 tutor often sings multiple motifs within a single bout, thus some motifs precede (and follow)  
 571 the alignment time. Error bars indicate mean  $\pm$  SEM.

572



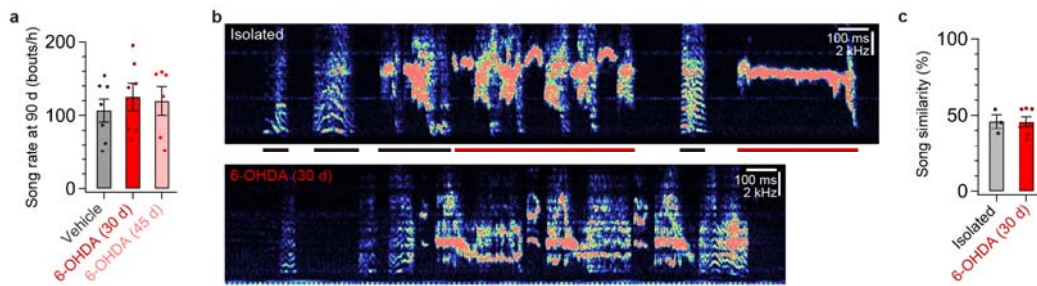
573

574 **Extended Data Figure 3 | Effects of 6-OHDA injection into HVC on DA fibers in HVC**  
 575 **and surrounding regions and on noradrenergic/adrenergic fibers in HVC**

576 **a**, From left to right, a max-projected image of serial sagittal sections visualized with a confocal

577 microscope, showing HVC with TH immunolabeling (~2.4 mm lateral), HVC shelf and  
 578 caudolateral nidopallium (NCL) just ventral to HVC with TH immunolabeling (~2.4 mm  
 579 lateral), and HVC with dopamine beta-hydroxylase (DBH) immunolabeling (~2.4 mm lateral)  
 580 in control birds, which received injection of vehicle into HVC. Similar results were obtained  
 581 in 5 independently repeated experiments (orientation is similar to **b**). **b**, From left to right, a  
 582 max-projected image of serial sagittal sections visualized with a confocal microscope, showing  
 583 HVC with TH immunolabeling (~2.4 mm lateral), HVC shelf and NCL just ventral to HVC  
 584 with TH immunolabeling (~2.4 mm lateral), and HVC with DBH immunolabeling (~2.4 mm  
 585 lateral) in birds that received injection of 6-OHDA into HVC 2 days before tissue fixation.  
 586 Similar results were obtained in 4 independently repeated experiments (D: dorsal, R: rostral).  
 587 **c**, Density of TH-positive (TH+) fibers in HVC of control birds ( $n = 5$  hemispheres from 3  
 588 birds) was higher than that of birds that received injections of 6-OHDA 2 days before fixation  
 589 (Tukey-Kramer test:  $P = 0.002$ ) ( $n = 4$  hemispheres from 2 birds), and that of birds that received  
 590 injections of 6-OHDA ~60 days before fixation, as in Fig. 3b-c (Tukey-Kramer test:  $P = 0.002$ )  
 591 ( $n = 6$  hemispheres from 4 birds). **d**, Density of TH+ fibers in HVC shelf and NCL in control  
 592 birds ( $n = 5$  hemispheres from 3 birds), birds that received injection of 6-OHDA 2 days before  
 593 fixation ( $n = 4$  hemispheres from 2 birds), and birds that received injection of 6-OHDA ~60  
 594 days before fixation, as in Fig. 3b-c ( $n = 6$  hemispheres from 4 birds). **e**, Density of DBH-  
 595 positive (DBH+) fibers in HVC in control birds ( $n = 4$  hemispheres from 2 birds) and birds that  
 596 received injection of 6-OHDA 2 days before injection ( $n = 4$  hemispheres from 2 birds) was  
 597 not significantly different (two-sided unpaired  $t$ -test:  $t(7) = 0.379$ ,  $P = 0.716$ ). Error bars  
 598 indicate mean  $\pm$  SEM.

599

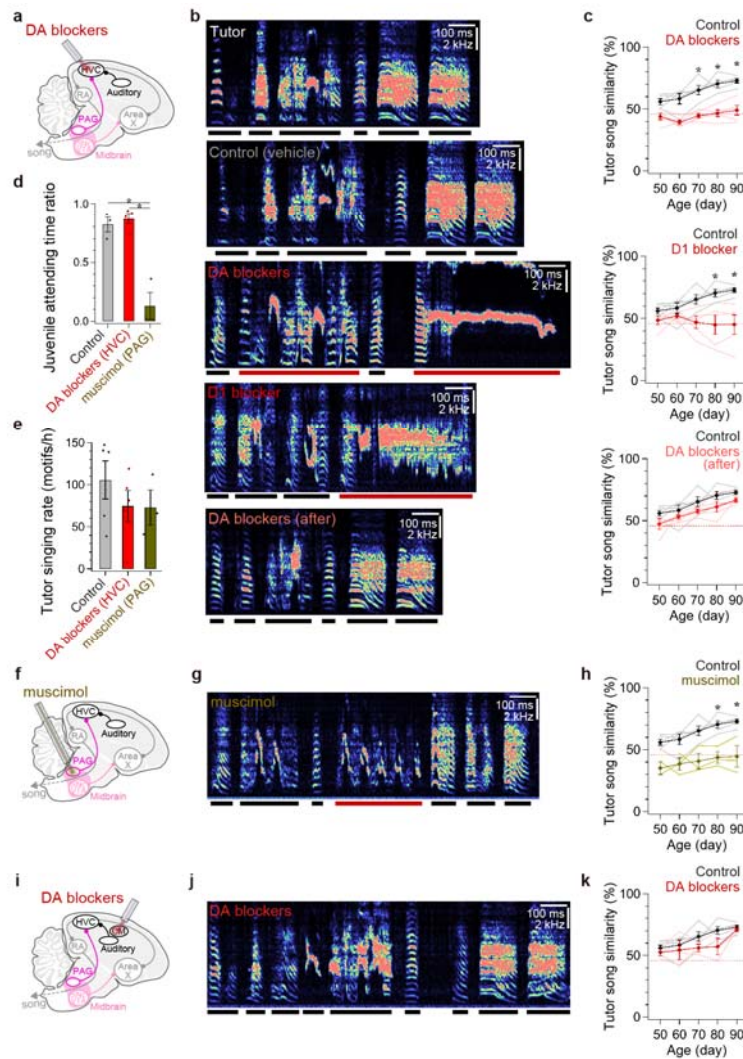


600

601 **Extended Data Figure 4 | Ablation of DA terminals in HVC did not affect song rate but**  
 602 **decreased song imitation to the level of birds raised in isolation from a tutor.**

603 **a**, The song rates of birds that received injection of vehicle ( $n = 7$ ), 6-OHDA at ~30 d ( $n = 7$ ),  
 604 and 6-OHDA at ~45 d ( $n = 6$ ) were not significantly different (one-way ANOVA:  $F(2,17) =$   
 605  $0.283$ ,  $P = 0.757$ ). **b**, Spectrograms from a 90-d bird that was raised in isolation from a tutor  
 606 (top) and from a 90-d bird that was normally tutored but received injection of 6-OHDA into  
 607 HVC at 30 d (bottom). **c**, Similarity of 90-d untutored (Isolated) birds' songs to songs of  
 608 unrelated adult zebra finches that had been normally tutored ( $n = 3$ ) was not significantly

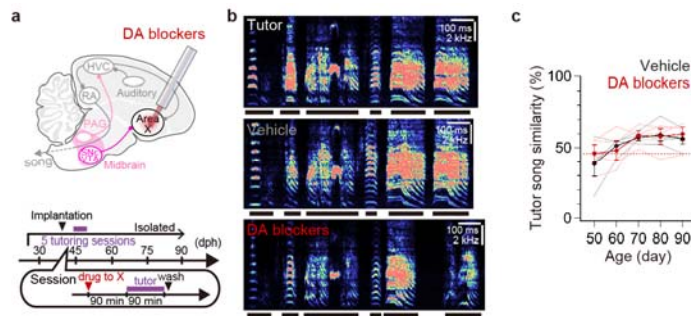
609 different from tutor song similarity of 90-d pupils that received injection of 6-OHDA into HVC  
 610 at ~30 d ( $n = 7$ ) (two-sided unpaired  $t$ -test:  $t(9) = 0.013$ ,  $P = 0.990$ ), but was significantly  
 611 different from tutor song similarity of 90-d pupils that received injection of vehicle at ~30 d ( $n$   
 612 = 7) ( $t(9) = 3.028$ ,  $P = 0.014$ ), or from tutor song similarity of 90-d pupils that received injection  
 613 of 6-OHDA into HVC at ~45 d ( $n = 6$ ) (two-sided unpaired  $t$ -test:  $t(8) = 3.314$ ,  $P = 0.011$ ) (song  
 614 data from birds injected with 6-OHDA into HVC at ~30 d is same as Fig. 3e; song similarity  
 615 data from birds injected in HVC with vehicle at ~30 d or 6-OHDA at ~45 d are not shown here  
 616 but are shown in Fig. 3f). Error bars indicate mean  $\pm$  SEM.  
 617



618  
 619 **Extended Data Figure 5 | Effects of infusing DA blockers into HVC or CM and infusing**  
 620 **muscimol into PAG on song copying.**  
 621 **a**, Schematics showing infusion of DA blockers into HVC. **b**, From top to bottom, sound  
 622 spectrograms of a song of a tutor bird, a 90-d pupil that received infusion of vehicle during  
 623 tutoring sessions, a 90-d pupil that received infusion of both D1- and D2-type DA blockers

624 (DA blockers) during tutoring sessions, a 90-d pupil bird that received infusion of D1-type  
 625 blocker during tutoring sessions, and 90-d pupil that received infusion of both D1- and D2-  
 626 type DA blockers after tutoring sessions. **c**, Developmental changes in tutor song similarity of  
 627 pupils that received infusion of both D1- and D2-type DA blockers (DA blockers) into HVC  
 628 during tutoring sessions (top,  $n = 5$ ), a D1-type blocker into HVC during tutoring sessions  
 629 (middle,  $n = 5$ ), or DA blockers into HVC immediately after tutoring sessions (bottom,  $n = 5$ ).  
 630 Asterisks indicate  $P < 0.050$  with Tukey-Kramer test (See Methods). **d**, Proportion of time that  
 631 juvenile birds attended to the tutor during tutoring sessions was not significantly different  
 632 between birds that received vehicle ( $n = 3$ ) or DA blockers into HVC ( $n = 4$ ) (Tukey-Kramer  
 633 test:  $P = 0.871$ ). The attention time of juvenile birds that received infusion of muscimol into  
 634 PAG ( $n = 3$ ) was lower than that of control birds (Tukey-Kramer test:  $P = 0.001$ ) and that of  
 635 birds that received injection of DA blockers into HVC (Tukey-Kramer test:  $P < 0.001$ ). **e**,  
 636 Singing rates of the tutor bird to pupils that received vehicle into HVC ( $n = 5$ ) were not different  
 637 from that to pupils that received injection of DA blockers into HVC ( $n = 5$ ) or muscimol into  
 638 PAG ( $n = 3$ ) (one-way ANOVA:  $F(2,10) = 0.776$ ,  $P = 0.486$ ). **f**, Schematics showing infusion  
 639 of muscimol into PAG. **g**, A sound spectrogram of a song of a 90-d pupil that received infusion  
 640 of muscimol into PAG during tutoring sessions. A sound spectrogram of the tutor song is shown  
 641 in **b**. **h**, Tutor song similarity of pupil birds that received infusion of vehicle into HVC and  
 642 birds that received infusion of muscimol blockers into PAG were significantly different (Tukey-  
 643 Kramer test: vehicle:  $n = 5$ , muscimol to PAG:  $n = 3$ ; at 90 d:  $P = 0.007$ ). **i**, Schematics showing  
 644 infusion of DA blockers into CM (DA blockers possibly diffused into both the medial and  
 645 lateral CM). **j**, A sound spectrogram of a song of a 90-d pupil that received infusion of DA  
 646 blockers into CM during tutoring sessions. A sound spectrogram of the tutor song is shown in  
 647 **b**. **k**, Tutor song similarity of pupil birds that received infusion of vehicle into HVC and birds  
 648 that received infusion of DA blockers into CM were not significantly different (Tukey-Kramer  
 649 test: vehicle:  $n = 5$ , DA blockers to CM:  $n = 3$ ; at 90 d:  $P = 1.000$ ). Horizontal red dashed lines  
 650 in **c**, **h**, and **k** show song similarity between 90-d untutored birds and unrelated adult male zebra  
 651 finches that had been raised with normal exposure to a tutor (See Extended Data Fig. 4b-c).  
 652 Error bars indicate mean  $\pm$  SEM.

653



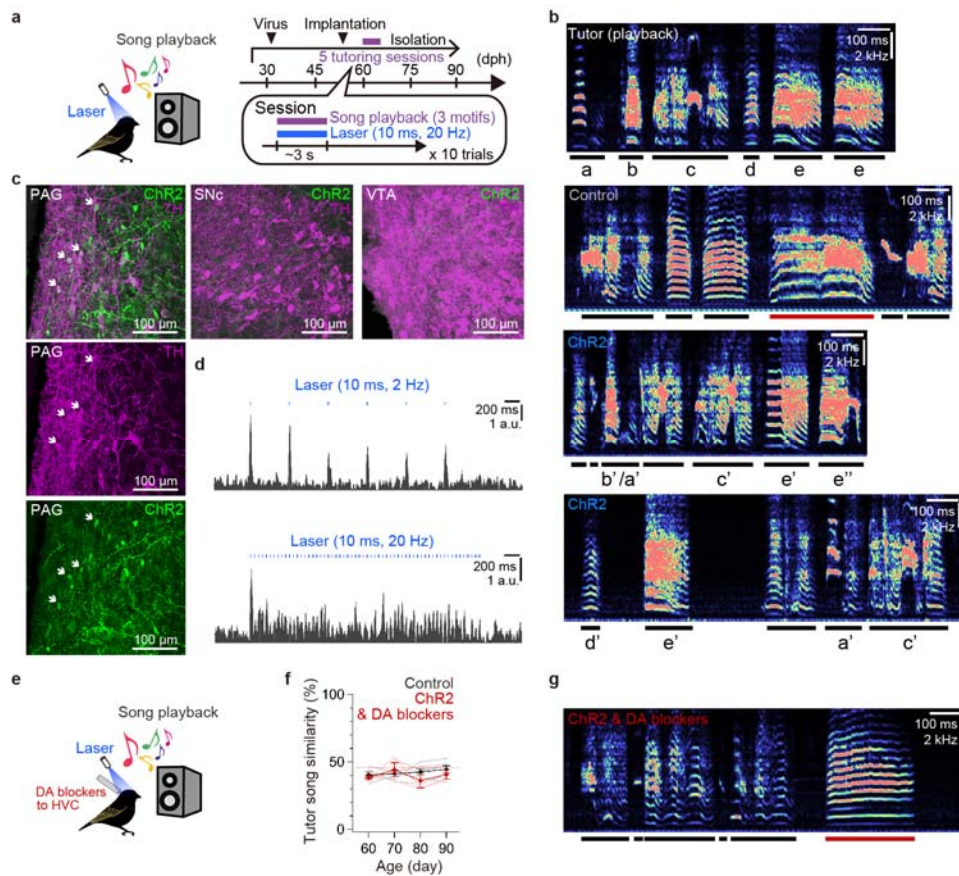
654

655

**Extended Data Figure 6 | Infusion of DA blockers into Area X in juvenile males did not**

656 **disrupt song copying.**

657 **a**, Schematics (top) and schedule (bottom) of infusion of DA blockers into Area X. **b**, Sound  
 658 spectrograms of a song of a tutor (top), a 90-d bird that received infusion of vehicle into Area X  
 659 X during tutoring sessions (middle), and a 90-d bird that received infusion of DA blockers into  
 660 Area X during tutoring sessions (bottom). **c**, Tutor song similarity of pupil birds that received  
 661 infusion of vehicle into Area X and birds that received infusion of DA blockers into Area X  
 662 were not significantly different (Tukey-Kramer test: vehicle:  $n = 4$ , DA blockers:  $n = 4$ ; at 90  
 663 d:  $P = 1.000$ ). The horizontal red dashed line shows song similarity between 90-d untutored  
 664 birds and unrelated adult male zebra finches that had been raised with normal exposure to a  
 665 tutor (See Extended Data Fig. 4b-c). Error bars indicate mean  $\pm$  SEM.

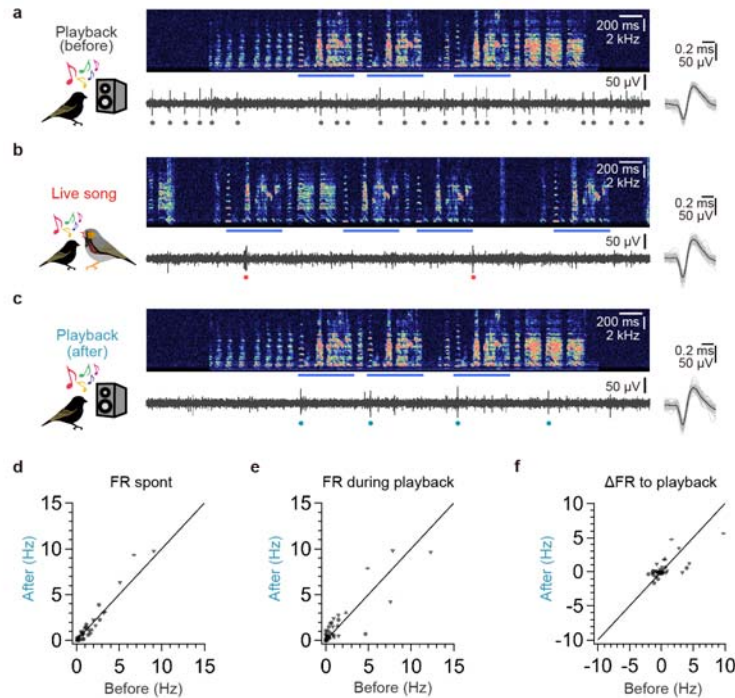


667

668 **Extended Data Figure 7 | Optogenetic activation of PAG<sub>HVC</sub> terminals paired with song**  
 669 **playback.**

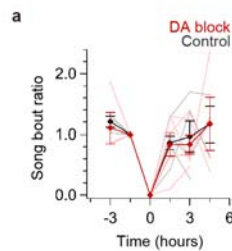
670 **a**, Schematics (left) and schedule (right) of optogenetic stimulation of PAG<sub>HVC</sub> terminals paired  
 671 with song playback. **b**, Sound spectrograms of song playback used in tutoring sessions (top), a  
 672 song of a 90-d pupil tutored by song playback without viral injection and laser stimulation  
 673 (upper middle), and 90-d pupils that received activation of PAG<sub>HVC</sub> terminals paired with song  
 674 playback (lower middle and bottom). **c**, From left to right, a max-projected image of serial

675 sagittal sections of PAG (left, ~0.5 mm lateral), showing PAG neurons expressing both ChR2  
 676 (green) and TH (pseudo-colored magenta) (arrows), SNc (middle, ~0.8 mm lateral), and VTA  
 677 (right, ~0.3 mm lateral). Similar results were obtained in 6 independently repeated experiments.  
 678 **d**, Multiunit activity in PAG, showing time-locked response to laser stimulation at 2 Hz (top)  
 679 and 20 Hz (bottom). **e**, Schematics of optogenetic stimulation of PAG<sub>HVC</sub> terminals paired with  
 680 song playback while infusing DA blockers into HVC. **f**, Tutor song similarity of pupils that  
 681 received activation of PAG<sub>HVC</sub> terminals paired with song playback while infusing DA blockers  
 682 into HVC (red,  $n = 3$ ) was not different from control birds shown in Fig. 3j (Tukey-Kramer  
 683 test: at 90 d:  $P = 1.000$ ), but lower than that received activation of PAG<sub>HVC</sub> terminals paired  
 684 with song playback shown in Fig. 3j (Tukey-Kramer test: at 90 d:  $P = 0.019$ ). **g**, A sound  
 685 spectrogram of a 90-d pupil that received optogenetic activation of PAG<sub>HVC</sub> terminals paired  
 686 with song playback while infusing DA blockers into HVC. A sound spectrogram of the song  
 687 playback used in tutoring sessions is shown in **b**. Error bars indicate mean  $\pm$  SEM.  
 688



689 **Extended Data Figure 8 | Spike activity of HVC neurons in juvenile male zebra finches**  
 690 **before and after their first exposure to live tutor songs.**  
 691 **a-c**, Action potential activity of an HVC neuron to tutor song playback before exposure to a  
 692 singing tutor (**a**), to live tutor songs (**b**), and to tutor song playback after exposure to live tutor  
 693 songs (**c**) (top: sound spectrogram, bottom: voltage recording, bottom right: exemplar 50 spikes  
 694 [gray] and their average [black]. circle: individual spike. blue bar: tutor song motif). **d**,  
 695 Spontaneous firing rate (FR spont) of HVC neurons of juvenile males before and after exposure  
 696 to live tutor songs (two-sided paired  $t$ -test: Mean FR. Before:  $1.6 \pm 0.3$  Hz; After:  $1.6 \pm 0.4$  Hz;  
 697

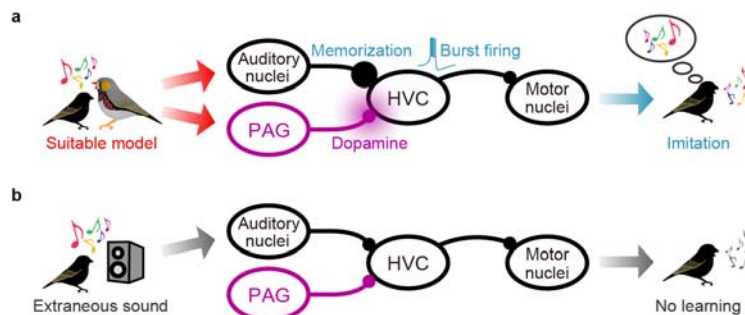
698  $t(34) = 0.794, P = 0.433, n = 35, 4$  birds). **e**, Firing rate of juvenile male HVC neurons during  
 699 playback of tutor songs (FR during playback) before and after exposure to live tutor songs  
 700 (two-sided paired  $t$ -test: Mean FR. Before:  $2.0 \pm 0.6$  Hz; After:  $2.1 \pm 0.6$  Hz;  $t(34) = 0.468, P$   
 701  $= 0.643, n = 35, 4$  birds). **f**, Changes in firing rate ( $\Delta$ FR) of juvenile HVC neurons in response  
 702 to playback of tutor songs before and after exposure to live tutor songs (two-sided paired  $t$ -  
 703 test: $\Delta$ FR. Before:  $0.5 \pm 0.4$  Hz; After:  $0.5 \pm 0.2$  Hz;  $t(34) = 0.079, P = 0.937, n = 35, 4$  birds).  
 704



705

706 **Extended Data Figure 9 | Song rates of juvenile birds before and after their first tutoring**  
 707 **sessions.**

708 **a**, Ratio of song bouts produced before and after the first tutoring session in control birds (black,  
 709  $n = 6$ ) and in birds that received injection of 6-OHDA injections into HVC several days prior  
 710 to the tutoring session or that were infused with DA blockers into HVC immediately before  
 711 and during the tutoring session (red,  $n = 6$ ). Error bars indicate mean  $\pm$  SEM.  
 712



713

714 **Extended Data Figure 10 | Summary diagram.**

715 **a**, The song of a live adult tutor (i.e., a suitable model) activates auditory afferents and DA-  
 716 releasing PAG afferents to HVC, leading to potentiation and stabilization of auditory synapses  
 717 in HVC. This plastic change forms temporally precise coding of the tutor songs and increases  
 718 the occurrence of bursting activity in HVC, which rapidly alters temporal and spectral features  
 719 of the pupil's vocalization in manner that drives imitation. **b**, Playback of an adult male song  
 720 without social cues (i.e., extraneous sound) only activates auditory afferents in HVC. The  
 721 activation of these auditory inputs by itself can neither alter HVC activity nor drive song  
 722 learning, similar to the condition where DA signaling in the pupil's HVC is blocked during the  
 723 juvenile's exposure to a live, singing tutor.





725 **Supplementary Video 1 | Social interaction of a pupil with vehicle in HVC**  
726 Social interaction of a juvenile bird that received infusion of vehicle into HVC during a tutoring  
727 session.  
728 <https://www.dropbox.com/s/xzftjq1z8ebutg/>  
729

730 **Supplementary Video 2 | Social interaction of a pupil with DA blockers in HVC**  
731 Social interaction of a juvenile bird that received infusion of DA blockers into HVC during a  
732 tutoring session.  
733 <https://www.dropbox.com/s/u7faje7dgawptpi/>  
734

735 **Supplementary Video 3 | Social interaction of a pupil with muscimol in PAG**  
736 Social interaction of a juvenile bird that received infusion of muscimol into PAG during a  
737 tutoring session.  
738 <https://www.dropbox.com/s/9vy9pkgh52vuc0i/>  
739